Journal of Alloys and Compounds 509 (2011) 6731–6735

Contents lists available at ScienceDirect

Journal of Alloys and Compounds

journal homepage: www.elsevier.com/locate/jallcom

Diphenylthiocarbazone (dithizone)-assisted solvothermal synthesis and optical properties of one-dimensional CdS nanostructures

Jing Zhou, Gaoling Zhao*, Jinjian Yang, Gaorong Han*

State Key Laboratory of Silicon Materials and Department of Materials Science and Engineering, Zhejiang University, Hangzhou 310027, PR China

ARTICLE INFO

Article history:
Received 17 December 2010
Received in revised form 28 March 2011
Accepted 29 March 2011
Available online 5 April 2011

Keywords:
Nanostructured materials
Chemical synthesis
Optical properties

ABSTRACT

One-dimensional (1D) cadmium sulfide (CdS) nanostructures with various aspect ratios were successfully synthesized by a diphenylthiocarbazone (dithizone)-assisted solvothermal method. The results showed that the dithizone-assisted synthesized samples had larger aspect ratio than that prepared in the absence of dithizone, and CdS nanowires with the highest aspect ratio were obtained with an appropriate dithizone amount (0.03 g/50 ml ethylenediamine in the present system). All the 1D CdS nanostructures were in hexagonal wurtzite phase. The as-synthesized large-scale CdS nanowires were in diameters ranging from 70 to 80 nm, length up to 20 μm, and aspect ratios of 250–285. Further characterization indicated that the CdS nanowires were single crystalline with a preferential growth orientation of [0 0 2], *c*-axis. Two optical absorption peaks were observed at about 488 nm and 502 nm for the CdS nanowire sample with high aspect ratio in the optical absorption spectroscopy, which could be attributed to the nanometer effect of nanowires. It was found that the additive dithizone was a crucial factor in controlling the morphology and optical properties of the 1D CdS nanostructures. The growth mechanism of 1D CdS nanostructure and the effects of dithizone in the present system were discussed.

1. Introduction

During the past decades, one-dimensional (1D) semiconductor nanomaterials have attracted much attention due to their electronic, optical, chemical properties as well as their potential applications in nanoscale electronic and optoelectronic devices [1–5]. As a direct band gap material with E_g of 2.42 eV at room temperature, cadmium sulfide (CdS) is one of the most important semiconductors for the extensive application in light-emitting diodes, solar cells, and other optoelectronic devices [6–10]. Various techniques, such as vapor–liquid–solid (VLS) growth, chemical vapor deposition (CVD), and thermal evaporation, have been developed to synthesize 1D CdS nanostructures [11–13]. However, the above-mentioned methods usually require special instruments, high vacuum or high temperature.

On the other hand, the solvothermal method is a simple, low-cost and highly efficient synthetic approach for the preparation of 1D CdS nanostructures, and the process could be easily controlled [14–17]. Although many efforts have been made on the synthesis of CdS nanowires, further studies on fabricating single crystalline CdS nanowires with high aspect ratio are still necessary for widespread application. It has been reported that the growth of semiconductor nanorods or nanowires significantly depends on the additives in the solvothermal process [18–20]. Moreover, the optical, electrical, as well as other properties of 1D semiconductor nanostructures are found to be very sensitive to the additives [18–21]. For instance, Wang et al. [18] found that CdS nanorods synthesized by poly(vinyl-alcohol) (PVA)-assisted solvothermal method showed larger aspect ratio than the sample prepared without PVA, and the dosage of PVA played an important role in the morphology and optical properties of CdS nanorods. Kang et al. [21] reported that the anisotropic elongation of CdS nanowires can be enhanced by optimizing the type of surfactants and their respective molar ratio in the solution-based synthesis. Therefore choosing the additive is one of the key issues for the solvothermal synthesis of 1D CdS nanostructures. Diphenylthiocarbazone (dithizone) has two big π bonds in its module and is considered to have the ability to transport carrier. In our previous work, it has been verified that CdS nanorods synthesized with dithizone as the additive through chemical bath deposition showed enhanced electrical properties [22]. This encourages us to do further research on the formation of CdS nanowires via a dithizone-assisted solvothermal process.

In this paper, CdS nanowires were synthesized by solvothermal method using dithizone as an additive. The growth process of the 1D CdS nanostructures and the effects of dithizone on the formation of CdS were discussed. The optical absorption properties of the as-prepared 1D CdS nanomaterials were also investigated.

* Corresponding authors. Tel.: +86 571 87952341; fax: +86 571 87952341.
E-mail address: glzhao@zju.edu.cn (G. Zhao).

0925-8388/$ – see front matter © 2011 Elsevier B.V. All rights reserved.
doi:10.1016/j.jallcom.2011.03.159

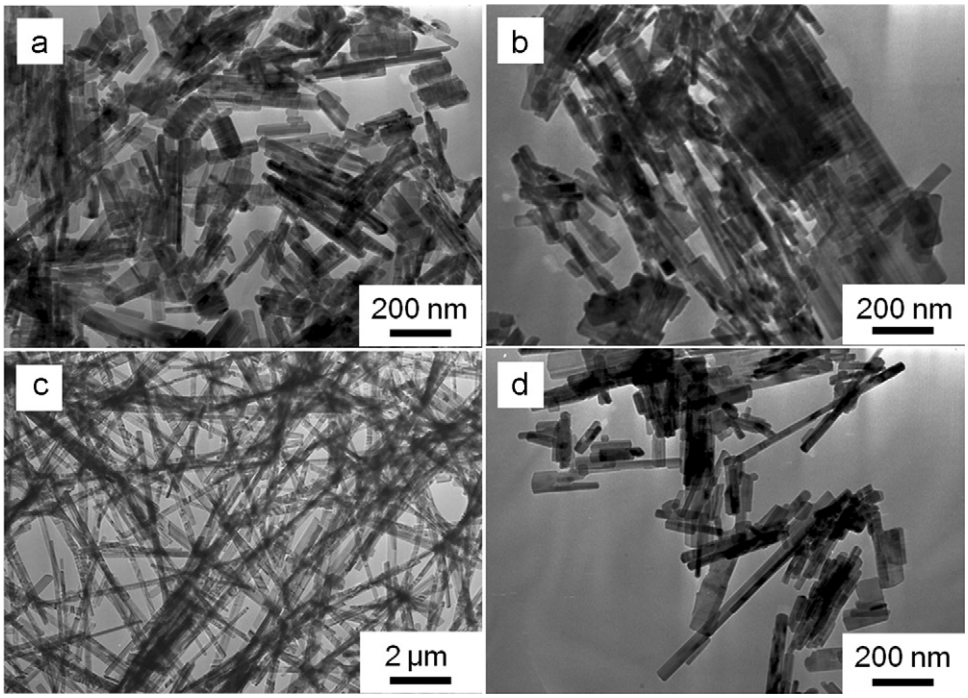

Fig. 1. Typical TEM images of the samples synthesized with various dithizone amounts of (a) 0 g/50 ml en, (b) 0.01 g/50 ml en, (c) 0.03 g/50 ml en, and (d) 0.05 g/50 ml en.

2. Experimental

Cadmium chloride ($CdCl_2$), thiourea (H_2NCSNH_2), dithizone ($C_{13}H_{12}N_4S$) and ethylenediamine (en) ($H_2NCH_2CH_2NH_2$) were used as the Cd source, S source, additive and solvent, respectively. All the chemicals were analytical pure and used without further purification. Cadmium chloride (1 mmol), thiourea (3 mmol) and dithizone (0, 0.01, 0.03, or 0.05 g) were put into a 62.5 ml Teflon-lined autoclave. Then 50 ml of en was added into the autoclave. The autoclave was sealed and maintained at 180 °C for 4 days. Then it was cooled to room temperature. The yellow products were collected and washed repeatedly with distilled water and ethanol to remove the by-products. The final products were dried in a vacuum oven at 50 °C.

X-ray diffraction (XRD) measurements were carried out with a D/max-RA model X-ray diffractometer equipped with a Cu Kα radiation (λ = 1.54 Å). The field emission scanning electron microscope (FESEM) images and X-ray energy dispersion analysis (EDAX) of the samples were recorded using a FEI-SIRION microscopy. Transmission electron microscopy (TEM) and selected area electron diffraction (SAED) were performed on a JEM-100CXII TEM operated at 160 kV. High resolution transmission electron microscope (HRTEM) was recorded on a CM200 HRTEM at 200 kV. Fourier transform infrared (FTIR) absorption spectra were obtained by a Nicolet-Avatar 360 spectrometer. The optical absorption spectra were measured by a Perkin-Lamba-20 UV–vis spectrophotometer.

3. Results and discussion

3.1. Effects of dithizone on the microstructures of 1D CdS nanostructures

Fig. 1 shows the typical TEM images of the CdS samples synthesized with various dithizone amounts. It is revealed that sample prepared in the absence of dithizone has a short and irregular rodlike shape with diameters in the range of 15–35 nm and lengths of 40–380 nm (Fig. 1a). When a small amount of dithizone (0.01 g/50 ml en) is added, the rods show a higher aspect ratio with diameters of 26–40 nm and lengths of 35–600 nm (Fig. 1b). Fig. 1c shows the TEM image of the sample derived from the dithizone amount of 0.03 g/50 ml en, which presents a nanowire-shaped structure with diameters ranging from 70 to 80 nm, length up to 20 μm, and aspect ratios of 250–285. Further increasing the dithizone amount to 0.05 g/50 ml en, the sample possesses an irregular rod morphology with an average diameter of 18 nm and lengths of 110–880 nm (Fig. 1d), indicating the aspect ratio of the 1D structure decreases.

Fig. 2 shows the XRD patterns of the as-synthesized samples with various dithizone amounts. All the strong and sharp diffraction peaks can be indexed to hexagonal wurtzite CdS phase (JCPDS card No. 41-1049). No diffraction from impurities could be detected, indicating the high purity of the synthesized samples. During the XRD measurements, the angles of incidence and reflection from the specimen surface are equal. Consequently, only crystal planes (*h k l*) parallel with the surface produce observable diffraction peaks. Nanowires lying parallel with the XRD specimen surface, therefore only crystal planes parallel with the growth axis contribute to diffraction peaks [23–25]. For the sample prepared without dithizone (Fig. 2a), the (0 0 2) reflection appears more intense and narrower than those of (1 0 0) and (1 0 1), indicating that the rod-shaped crystals has a growth direction of [0 0 2] [26–28]. With

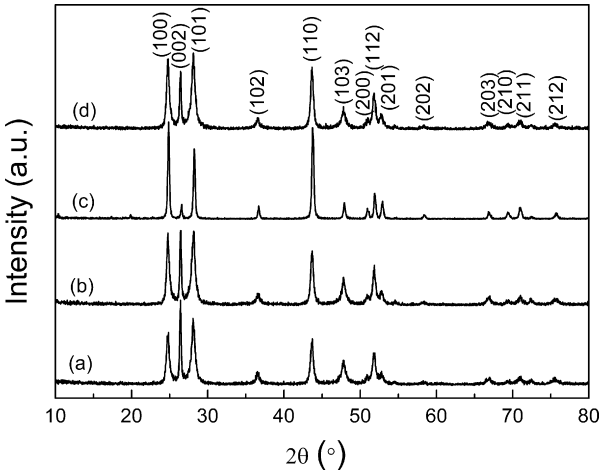

Fig. 2. XRD patterns of the samples synthesized with various dithizone amounts of (a) 0 g/50 ml en, (b) 0.01 g/50 ml en, (c) 0.03 g/50 ml en, and (d) 0.05 g/50 ml en.

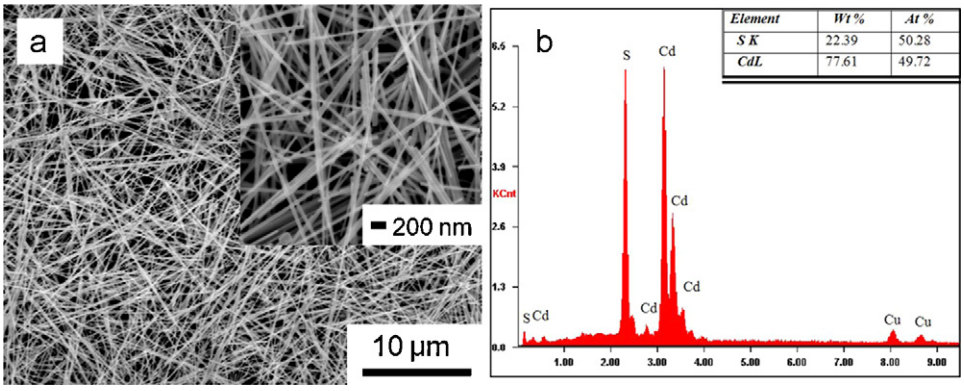

Fig. 3. Typical SEM image (a) and corresponding EDAX pattern (b) of CdS nanowires derived from the dithizone amount of 0.03 g/50 ml en.

increasing dithizone amount (Fig. 2b and c), the intensities of (1 0 0) and (1 0 1) peaks enhance, while that of (0 0 2) peak decreases, suggesting the (1 0 0) and (1 0 1) peaks increase at faster rates than the (0 0 2) peak. Compared with the standard card, the diffraction peaks of (1 0 0) and (1 1 0) are relatively strong, while the peak of (0 0 2) is weak. This can be ascribed to two factors as follows: the CdS nanorods or nanowires have a preferential orientation along the *c*-axis, and they lie mostly with their *c*-axis parallel with the experimental plane in the XRD measurement process [23,29]. This orientation growth can be further demonstrated below by HRTEM and SAED analysis. For the sample synthesized from further increasing dithizone amount (Fig. 2d), the (0 0 2) peak intensity increases and the (1 0 0) and (1 0 1) peak intensity slightly declines compared with that in Fig. 2c, which is due to the rod shape and lower aspect ratio. The intensity distribution in XRD profiles indicates that the additive dithizone benefits to the formation of high aspect ratio nanowires.

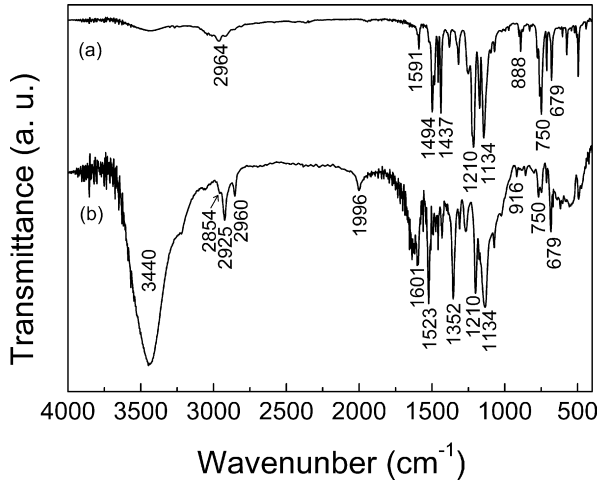

Fig. 5. FTIR spectra of pure dithizone (a) and the CdS nanowires derived from the dithizone amount of 0.03 g/50 ml en (b).

3.2. Further characterization and formation mechanism of CdS nanowires

Typical SEM image of CdS nanowires derived from the dithizone amount of 0.03 g/50 ml en is shown in Fig. 3a. It further confirms that large quantities of uniform nanowires are obtained, possessing a diameter in the range of 70–80 nm, length up to 20 μm, and aspect ratios of 250–285. In order to testify the chemical composition of the synthesized nanowires, EDAX analysis is carried out as shown in Fig. 3b. It indicates that the synthesized nanowire is only composed of Cd and S (the Cu peak responds to the copper sample stage). The atomic ratio of cadmium to sulfur is 49.72 to 50.28, which is close to the stoichiometric ratio of 1:1, illustrating the high purity of the synthesized CdS nanowires.

Further information about the microstructure of the as-prepared CdS nanowires derived from the dithizone amount of 0.03 g/50 ml en is provided by TEM, HRTEM images and SAED pattern. Fig. 4a shows the typical TEM image of an individual CdS nanowire, revealing that the CdS nanowire is straight with a uni-

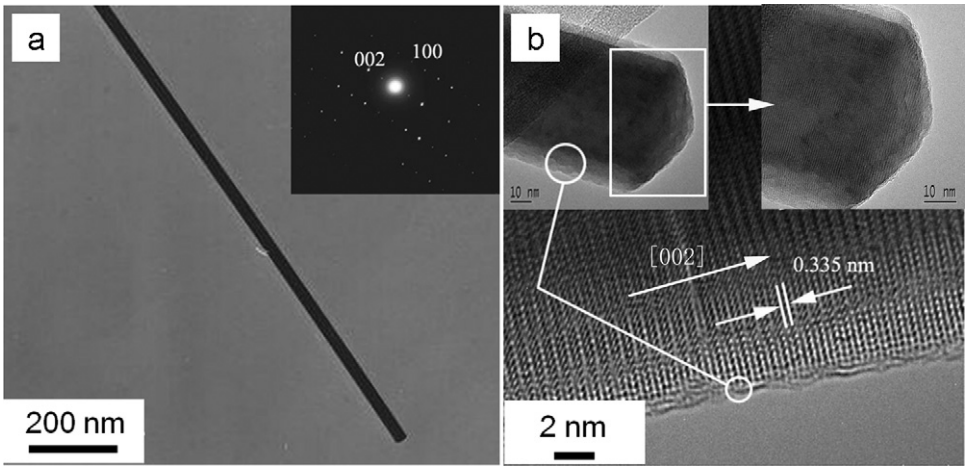

Fig. 4. (a) Typical TEM image and the corresponding SAED pattern (inset) of a single CdS nanowire derived from the dithizone amount of 0.03 g/50 ml en. (b) HRTEM image of the corresponding CdS nanowire in (a) Insets: overview (upper-left corner) and enlarged images (upper-right corner) of the tip of the nanowire.

form diameter of 70 nm. The corresponding SAED pattern is shown in the top-right-hand corner of Fig. 4a, indicating that the CdS nanowire is single crystalline with preferential growth direction of [0 0 2]. HRTEM image of the CdS nanowire is given in Fig. 4b. The measured interplanar spacing between adjacent lattice planes is 0.335 nm, which corresponds to the distance of (0 0 2) crystal planes, affirming that [0 0 2], *c*-axis, is the preferential growth orientation for as-prepared CdS nanowires. As shown both in the enlarged sides (marked circles) and tip of the nanowire (marked square frame) in Fig. 4b, it is worthy of notice that the CdS nanowire is coated with an amorphous layer especially on the side faces, which might be ascribed to the adsorbed additive dithizone.

The FTIR spectra of pure dithizone and the CdS nanowires derived from the dithizone amount of 0.03 g/50 ml en are shown in Fig. 5. In the FTIR pattern of the CdS nanowires, the 3440 cm^{-1} peak is the stretching vibration mode of N–H bond. Three well-resolved peaks at 2854, 2925, and 2960 cm^{-1} are assigned to methylene C–H symmetric, methylene C–H antisymmetric, and methyl asymmetric vibrational absorption bands, respectively. In pure dithizone, the absorption peaks at 1494 and 1591 cm^{-1} are attributed to the benzene ring stretching band, whereas in the spectrum of CdS nanowires, these peaks shift to 1523 and 1601 cm^{-1} due to the formation of Cd–N bond in Cd–N–C_6H_5. In dithizone, the peak at 1437 cm^{-1} corresponds to the C=S stretching mode, while the peak shifts to 1352 cm^{-1} for CdS nanowires due to the introduction of Cd in C=S–Cd. The peak at 1210 cm^{-1} is assigned to the deformation vibration of N–H bond. Compared with its relative intensity in dithizone, it declines in CdS nanowires due to the substitution of Cd for H ion in one of N–H bonds for one dithizone molecule. The peak at 1134 cm^{-1} is attributed to the C–H inplane bending vibration of benzene ring. In pure dithizone, the peak at 888 cm^{-1} corresponds to the N–N stretching mode, while in the spectrum of CdS nanowires, the peak shifts to 916 cm^{-1} due to the introduction of Cd–N bond in Cd–N–C_6H_5. The peaks at 679 and 750 cm^{-1} are ascribed to the benzene ring deformation vibration mode. The FTIR results indicate that dithizone is chelated on the as-obtained CdS nanowires, which is in agreement with the HRTEM image.

Based on the above-mentioned results, the growth process of the as-synthesized 1D CdS nanostructures can be expressed as follows:

$$Cd^{2+} + 2en \rightarrow [Cd(en)_2]^{2+} \quad (1)$$

$$(NH_2)_2CS + 2H_2O \rightarrow 2NH_3 + H_2S + CO_2 \quad (2)$$

$$[Cd(en)_2]^{2+} + S^{2-} \rightarrow CdS + 2en \quad (3)$$

The complexation reaction between Cd^{2+} and the solvent en occurs first, obtaining $[Cd(en)_2]^{2+}$ complex compound in the solution (reaction (1)) [30,31]. At high temperature, S^{2-} decomposed from thiourea (reaction (2)) captures Cd^{2+} in $[Cd(en)_2]^{2+}$, composing CdS nanocrystalline (reaction (3)) [30]. CdS nanocrystallites preferentially grow along *c*-axis in the existence of en [32,33]. It is worthy mentioned that, as a widely used solvent in the synthesis of nanocrystalline, en is believed to play following roles in the present system: (1) provide reaction environment that can not only greatly enhance solubility, diffusion, and crystallization but also be mild enough to let molecular building blocks participate solid-state phase in the solvothermal process [34]; (2) form symmetric bidentate ligand complex with cadmium ion and guide the growth direction, *c*-axis [32,35].

Meanwhile, dithizone chelates on the surface of the synthesized CdS nanostructures, which can be confirmed by HRTEM and FTIR results (see Figs. 4b and 5). The cheletropic reaction between dithizone and Cd^{2+} can be described as reaction (4), obtaining the ligand complex, $[Cd(dithizone)]^+$:

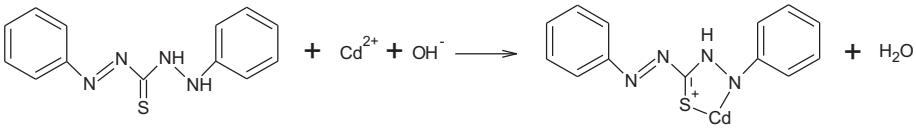

(4)

The stability of the $[Cd(dithizone)]^+$ complex is expected to decrease with increasing temperature [33]. At higher reaction temperature, S^{2-} may coordinate to $[Cd(dithizone)]^+$ complex and the volatile dithizone molecules deplete gradually, resulting in the formation of CdS nanostructures [33,36]. It is believed that the intermediate ligand complex has a tendency to selectively bind strongly to preferential crystallographic planes and as a consequence could serve as the soft molecular template for anisotropic growth of nanocrystals [36,37]. According to the previous report [18,36–39] and also confirmed by our HRTEM images (see Fig. 4b), it can be inferred that dithizone has stronger interaction with the side face of the nanorods or nanowires than that with the ends of the *c*-axis direction. Once nucleation starts, the selective facets of small nucleus, i.e., the lateral faces, are capped by the ligand complex layer, inhibiting the growth of the lateral faces [36]. Meanwhile, S^{2-} may bond to Cd through the unoccupied facets of the seeded nucleus, i.e., the ends of *c*-axis, and consequently the preferential growth orientation, *c*-axis, is advantaged.

Noticeably, for the sample in the absence of dithizone, only the solvent of en takes effect on the anisotropic growth, resulting in short nanorods with low aspect ratio (Fig. 1a). When a small amount of dithizone is added (0.01 g/50 ml en), the dithizone molecules adsorb on the nanocrystals, but are not enough for a complete layer on the side face, leading to a weak control of the nanostructure growth in the lengthwise direction (Fig. 1b) [18]. In the case that 0.03 g/50 ml en is added, uniform nanowires with high ratio aspect are obtained (Fig. 1c), indicating that the anisotropic growth of the 1D product is promoted in an appropriate amount of dithizone. The capped ligand complex layer serves as a molecular template, and the growth of CdS nanocrystalline prefers to copy their template's shape [39]. The growth on the lateral surface is inhibited by the capped dithizone layer, while that on the uncovered ends, *c*-axis, is preferentially enhanced, resulting in the formation of nanowires with high aspect ratio. However, too much dithizone is not favorable for the growth of high ratio aspect nanostructures, since the entire surface of the crystals might be covered by a dithizone layer, resulting in the inhibition of all orientation growth and consequently a rodlike shape with low aspect ratio (Fig. 1d) [18].

The above-mentioned experimental results and analysis demonstrate that the additive dithizone plays an important role in the growth of 1D CdS nanostructures, and that the crystal growth behavior is highly dependent on the dithizone amount in the present system.

3.3. Optical properties of 1D CdS nanostructures

Fig. 6 shows optical absorption spectra of the CdS samples synthesized with various dithizone amounts. Compared with the bandgap of the characteristic absorption of bulk CdS (513 nm), the optical absorption edges of all the samples have a blue shift due to the nanometer effect. Blue shift of the absorption peak is more obvious for the higher aspect ratio sample. For the CdS nanowires derived from the dithizone amount of 0.03 g/50 ml en, two absorption peaks at 502 nm (Peak L) and 488 nm (Peak S) are observed.

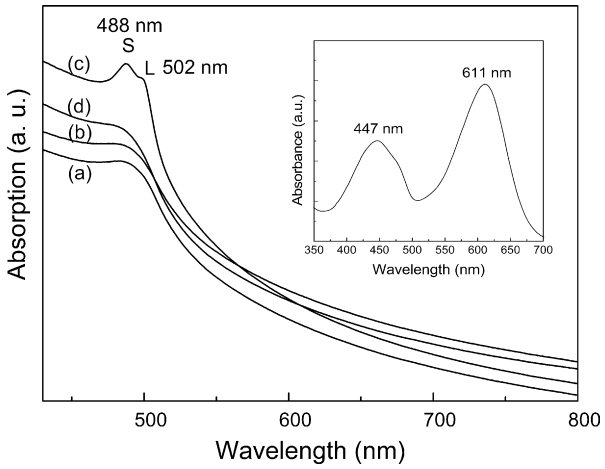

Fig. 6. Optical absorption spectra of the acetone solutions of CdS samples synthesized with various dithizone amounts of (a) 0 g/50 ml en, (b) 0.01 g/50 ml en, (c) 0.03 g/50 ml en, and (d) 0.05 g/50 ml en. The inset is the optical absorption spectrum of pure dithizone in acetone solution.

Considering the optical absorption peaks of dithizone at 447 nm and 611 nm as shown in the inset of Fig. 6, both Peaks L and S can be ascribed to the CdS nanowires. Based on the high aspect ratio and purity of CdS nanowire sample, Peaks L and S are suggested to be caused by the nanometer effect of the CdS nanowires.

It has been previously reported that the blue shift of the fundamental energy of semiconductor quantum wires depends on the lateral widths and shape when irradiated under fixed radiation conditions [40,41]. A blue shift of electron bound-state energy (first electron sub-band) of the quantum wires with decreasing lateral dimension can be observed. In contrast, at very large axial dimension, it gradually evolves into "bulky" character. For the sample produced with the dithizone amount of 0.03 g/50 ml en, the size in the lengthwise direction is on the micrometer scale while that in the radial direction is nano-size. Considering the electron bound-state energy differs in the lateral and axial dimensions, the optical absorption performances in the two directions occur at different wavelength. For a single CdS nanowire, the optical absorption peak in the radial direction has a blue shift compared with that in the lengthwise direction. Once the radius and length of the nanowires are uniform respectively, the extent of blue shift in optical absorption peak will be uniform. Consequently two peaks in the optical absorption spectrum occur as shown in curve (c) of Fig. 6.

4. Conclusions

1D CdS nanostructures have been successfully synthesized by solvothermal method using dithizone as the additive. The results indicate that the additive dithizone plays a vital role in controlling the morphology and optical properties of CdS nanostructures. Single crystalline CdS nanowires with uniform morphology and high aspect ratio could be obtained with an appropriate dithizone amount (0.03 g/50 ml en in this system). The prepared CdS nanowires exhibit unique optical absorption properties with two absorption peaks, which was due to the nanometer effect of the nanowires.

References

[1] M. Bruchez, M. Moronne, P. Gin, S. Weiss, A.P. Alivisatos, Science 281 (1998) 2013–2016.
[2] N. Fu, Z. Li, A. Myalitsin, M. Scolari, R.T. Weitz, M. Burghard, A. Mews, Small 6 (2010) 376–380.
[3] Q.C. Kong, R. Wu, X.M. Feng, C. Ye, G.Q. Hu, J.Q. Hu, Z.W. Chen, J. Alloys Compd. 509 (2011) 3048–3051.
[4] A.B. Djurisic, M.Y. Guo, M.K. Fung, F. Fang, X.Y. Chen, A.M.C. Ng, W.K. Chan, J. Alloys Compd. 509 (2011) 1328–1332.
[5] K.A. Razak, W.K. Tan, K. Ibrahim, Z. Lockman, J. Alloys Compd. 509 (2011) 820–826.
[6] Z.T. Deng, O. Schulz, S. Lin, B.Q. Ding, X.W. Liu, X.X. Wei, R. Ros, H. Yan, Y. Liu, J. Am. Chem. Soc. 132 (2010) 5592–5593.
[7] A.F.G. Monte, D. Rabelo, P.C. Morais, J. Alloys Compd. 495 (2010) 436–438.
[8] G.A. Zhu, T.A. Lv, L.K. Pan, Z. Sun, C.Q. Sun, J. Alloys Compd. 509 (2011) 362–365.
[9] Y.Z. Fan, M.H. Deng, G.P. Chen, Q.X. Zhang, Y.H. Luo, D.M. Li, Q.B. Meng, J. Alloys Compd. 509 (2011) 1477–1481.
[10] P. Chawla, S.P. Lochab, N. Singh, J. Alloys Compd. 509 (2011) 72–75.
[11] M. Lei, L.Q. Qian, Q.R. Hu, S.L. Wang, W.H. Tang, J. Alloys Compd. 487 (2009) 568–571.
[12] R. Agarwal, C.J. Barrelet, C.M. Lieber, Nano Lett. 5 (2005) 917–920.
[13] C.J. Barrelet, Y. Wu, D.C. Bell, C.M. Lieber, J. Am. Chem. Soc. 125 (2003) 11498–11499.
[14] X.X. Ren, G.L. Zhao, H. Li, W. Wu, G.R. Han, J. Alloys Compd 465 (2008) 534–539.
[15] M. Salavati-Niasari, D. Ghanbari, F. Davar, J. Alloys Compd. 492 (2010) 570–575.
[16] S.L. Xiong, B.J. Xi, Y.T. Qian, J. Phys. Chem. C 114 (2010) 14029–14035.
[17] R.S.S. Saravanan, D. Pukazhselvan, C.K. Mahadevan, J. Alloys Compd. 509 (2011) 4065–4072.
[18] H.M. Wang, P.F. Fang, Z. Chen, S.J. Wang, J. Alloys Compd. 461 (2008) 418–422.
[19] M. Salavati-Niasari, F. Davar, M.R. Loghman-Estarki, J. Alloys Compd. 481 (2009) 776–780.
[20] M. Jing, H.D. Gai, Z.G. Wang, K.S. Jiang, L.L. Wu, Y.S. Wu, Polym. Bull. 64 (2010) 413–419.
[21] C.C. Kang, C.W. Lai, H.C. Peng, J.J. Shyue, P.T. Chou, Small 3 (2007) 1882–1885.
[22] J. Zhou, G.L. Zhao, J.J. Yang, G.R. Han, Rare Metal. Mat. Eng. 39 (2010) 138–141.
[23] J. Puthussery, A.D. Lan, T.H. Kosel, M. Kuno, Acs Nano 2 (2008) 357–367.
[24] J.S. Jang, U.A. Joshi, J.S. Lee, J. Phys. Chem. C 111 (2007) 13280–13287.
[25] H.Q. Cao, G.Z. Wang, S.C. Zhang, X.R. Zhang, D. Rabinovich, Inorg. Chem. 45 (2006) 5103–5108.
[26] C. Wang, Y.H. Ao, P.F. Wang, J. Hou, J. Qian, S.H. Zhang, Mater. Lett. 64 (2010) 439–441.
[27] P. Bera, C.H. Kim, S. Il Seok, Solid State Sci. 12 (2010) 532–535.
[28] P. Thangadurai, S. Balaji, P.T. Manoharan, Mater. Chem. Phys. 114 (2009) 420–424.
[29] Q.Q. Wang, G. Xu, G.R. Han, J. Solid State Chem. 178 (2005) 2680–2685.
[30] F. Li, W.T. Bi, T. Kong, C.J. Wang, Z. Li, X.T. Huang, J. Alloys Compd. 479 (2009) 707–710.
[31] Y.C. Zhang, G.Y. Wang, X.Y. Hu, J. Alloys Compd. 437 (2007) 47–52.
[32] J.H. Zhan, X.G. Yang, D.W. Wang, S.D. Li, Y. Xie, Y. Xia, Y.T. Qian, Adv. Mater. 12 (2000) 1348–1351.
[33] Y.D. Li, H.W. Liao, Y. Ding, Y.T. Qian, L. Yang, G.E. Zhou, Chem. Mater. 10 (1998) 2301–2303.
[34] B. Li, Y. Xie, H.L. Su, Y.T. Qian, X.M. Liu, Solid State Ionics 120 (1999) 251–254.
[35] M. Chen, Y. Xie, Z.Y. Yao, X.M. Liu, Y.T. Qian, Mater. Chem. Phys. 74 (2002) 109–111.
[36] P. Bera, C.H. Kim, S.I. Seok, Solid State Sci. 12 (2010) 1741–1747.
[37] N. Moloto, M.J. Moloto, N.J. Coville, S.S. Ray, J. Cryst. Growth 311 (2009) 3924–3932.
[38] M. Chen, Y. Xie, J. Lu, Y.J. Xiong, S.Y. Zhang, Y.T. Qian, X.M. Liu, J. Mater. Chem. 12 (2002) 748–753.
[39] K. Wei, C. Lai, Y.J. Wang, J. Macromol. Sci. A 43 (2006) 1531–1540.
[40] F.Y. Qu, P.C. Morais, Phys. Lett. A 310 (2003) 460–464.
[41] J.M. Worlock, F.M. Peeters, H.M. Cox, P.C. Morais, Phys. Rev. B 44 (1991) 8923–8926.